STUDY ON DEPOSITION REGIMES AND MECHANICAL PROPERTIES OF WELD OVERLAY COATINGS FOR THE RESTORATION OF WORN AGRICULTURAL MACHINERY PARTS

/

ИЗСЛЕДВАНЕ НА РЕЖИМИТЕ НА НАНАСЯНЕ И НА МЕХАНИЧНИТЕ СВОЙСТВА НА НАВАРЪЧНИ ПОКРИТИЯ ПРИ ВЪЗСТАНОВЯВАНЕ НА ИЗНОСЕНИ ДЕТАЙЛИ ОТ ЗЕМЕДЕЛСКИ МАШИНИ

Daniel LYUBENOV[1], Zhivko KOLEV [2], Seher KADIROVA [3], Georgi KADIKYANOV [1]

[1] Ruse University "Angel Kanchev", Faculty of Transport / Bulgaria

[2] Ruse University "Angel Kanchev", Agrarian – Industrial Faculty / Bulgaria

[3] Ruse University "Angel Kanchev", Faculty of Electrical Engineering, Electronics and Automation / Bulgaria

Tel: +359 877 089537; E-mail: skadirova@uni-ruse.bg

DOI: https://doi.org/10.35633/inmateh-78-86

Keywords: *agricultural machinery, restoration, weld coatings, deposition regimes, microstructure, microhardness*

ABSTRACT

The stability limits of weld overlay deposition processes on worn surfaces of steel cylindrical parts from agricultural machinery were investigated. The microstructure of the deposited coatings was analyzed, and the main structural constituents were identified. The microhardness distribution across the coating depth was determined. Furthermore, the influence of key technological parameters on selected mechanical properties of the weld metal was examined. The obtained results enable the determination of optimal deposition regimes for the restoration of worn parts, with the aim of improving their wear resistance and operational reliability.

РЕЗЮМЕ

Изследвани са границите на стабилно протичане на процесите при нанасяне на наваръчни покрития върху износени повърхности на стоманени цилиндрични детайли от земеделски машини. Анализирана е микроструктурата на получените покрития и са представени основните структурни съставляващи. Определена е микротвърдостта в дълбочина на наварените слоеве. Изследвано е влиянието на основни технологични параметри върху някои механични свойства на наварения метал. Получените резултати позволяват определяне на оптимални режими за възстановяване на износени детайли с цел повишаване на тяхната износоустойчивост и експлоатационна надеждност.

INTRODUCTION

In developed countries and regions, policies related to reproduction play an increasingly important role and lead to sustainable development (*Jia-qi Shen et al, 2025*).

During the operation of agricultural machinery, damage and wear of various components frequently occur and must be addressed in a timely and systematic manner, as most mechanized agricultural operations must be performed within specific agrotechnical time windows *(Bujaczek et al., 2013; Yanhu Zhang et al., 2026)*. This requirement is particularly critical during harvesting periods *(Jialin Han et al., 2020; Jialin Han et al., 2022; Yaoguang Hu et al., 2020)*.

The prices of agricultural machinery, material and technical resources, and mechanized production are continuously increasing and remain high. Sometimes there are insufficient funds to purchase new machines, or the purchasing and delivery process takes a long time, which may disrupt the technological workflow. Therefore, the quality of maintenance and repair of the equipment is of particular importance (*Vorotnikov I. et al, 2019; Yaoguang Hu et al, 2019*).

Reducing maintenance and repair costs, and increasing the life of machinery lead to increased efficiency in agricultural production (*Pourdarbani R., 2019; Yipu Yao et al, 2021; Jialin Han et al, 2021*).

Since maintenance and repair costs represent a large share of the total costs of agricultural machinery, up-to-date information on this issue is of great importance for farm management (*Burose F. and Sauer N., 2011*).

Unlike other types of agricultural machinery costs, maintenance and repair costs are difficult to predict over time and calculate in advance (*Lips M. and Burose F., 2012*). These costs increase as the age of machinery and equipment increases (*Calcante A. et al, 2013*).

Cylindrical components constitute a significant proportion of elements in various types of machinery. Due to operating conditions and prolonged service, their working surfaces are subjected to wear, corrosion, fatigue damage, and other defects *(Zichao Yu et al., 2024)*. This degradation leads to a reduction in the reliability and service life of the machinery *(Popovych et al., 2017)*.

Recycling agricultural machinery requires the availability of the necessary equipment, methods and technologies (*Malykha E.F. et al, 2023*).

The choice of a rational method for the restoration and repair of machine parts is often a complex problem, the solution of which requires specific steps (*Voynash S.A. et al, 2017*).

Welding methods are widely used for the restoration of agricultural machinery components. In many cases, layers of weld metal are deposited onto worn working surfaces, providing wear resistance equal to or greater than that of the original material. Determining the optimal parameters of the weld overlay deposition process is of great importance, particularly with regard to the thermal loading of the restored components *(Winczek et al., 2020)*. High temperatures may lead to the development of residual stresses and deformations *(Meléndez-Morales et al., 2023)*.

To assess the influence of deposition process parameters and filler material, metallographic cross-sections are commonly prepared and analyzed *(Gehling et al., 2022)*.

This paper presents the results of determining the stability limits of weld overlay deposition processes applied to worn surfaces of agricultural machinery components. The interactions between process parameters are analyzed, and the resulting coatings are evaluated in terms of wear resistance and resistance to mechanical stresses.

MATERIALS AND METHODS

Method for determining the stability limits of weld deposition processes in a carbon dioxide shielding environment (with and without electrode wire vibrations) and under a flux layer

The magnitude of the welding current is of decisive importance for the quality of weld metal formation when applying different weld overlay techniques to worn agricultural machinery components. It depends on the appropriate combination of electrical and kinematic parameters, as the current may vary within relatively wide limits. Therefore, even for identical electrode dimensions and geometry, the stability limits of the process may differ significantly. Process stability is characterized by the absence of molten metal flow, uniform slag separation during submerged arc welding (SAW), and minimal fluctuations in the welding current. The latter parameter is quantitatively evaluated using the coefficient of weld deposition non-uniformity. Consequently, it is necessary to determine the permissible ranges of controllable parameters for each weld deposition method that ensure stable process conditions.

The experimental investigations were carried out under laboratory conditions at the University of Ruse. Low-carbon steel electrode wires (grade SV-08G2S) with diameters of Ø = 1.0, 1.2, 1.6, and 2.0 mm were used for the different weld deposition methods mentioned above. The weld deposition process was performed on cylindrical steel specimens made of medium-carbon structural steel (grade 45), with a diameter of D = 80 mm.

The experiments for each electrode wire diameter were conducted at constant deposition velocity and voltage, taking into account the specific characteristics of the respective weld deposition processes (Table 1). Each experiment under identical conditions was repeated three times, resulting in a total of 171 specimens.

The electrode wire was fed into the arc zone using a KILBERG-type welding head, allowing stepless adjustment of the feed rate within the limits of stable process operation. A DC power source (IZA-G500) was used. Flux type VL-78 and carbon dioxide (CO_2) were used as shielding media, depending on the deposition method.

Statistical data analysis was performed using IBM SPSS Statistics (v.19). Process stability was evaluated using linear regression analysis, while differences between methods were assessed using one-way ANOVA followed by Tukey's HSD test ($p < 0.05$).

Table 1

Deposition velocity and voltage for different weld deposition methods

Weld deposition method		
CO_2 shielding with wire vibrations	**CO_2 shielding without wire vibrations**	**Under flux layer**
Velocity of weld coating deposition V_{wcd} [m/min]		
1.0	1.1	0.8
Voltage of weld coating deposition U_{wcd} [V]		
20	22	28

Method for investigation of the microhardness and microstructure of weld overlay coatings

One of the main factors determining the durability of restored components is the variation of microhardness along the thickness of the deposited layer, as well as its microstructure and the proportion of individual structural constituents. A correlation exists between these factors and wear resistance, which strongly depends on the dominant wear mechanism. Since hardness can be quantitatively measured, its distribution across the coating thickness can be used to characterize wear resistance with sufficient accuracy.

When different arc welding deposition methods and process conditions are applied to worn surfaces of cylindrical machine components, optimal wear resistance is achieved at specific microstructural states characteristic of each case. The variation of microhardness and microstructure along the height of the deposited layer can therefore serve as indirect indicators of the durability of the restored surfaces, depending on the prevailing wear conditions.

A comparative analysis of the microhardness and microstructure of the deposited weld metal coatings was performed. To evaluate the influence of the aforementioned factors, metallographic cross-sections were prepared. These were obtained from specimens deposited under CO_2 shielding (with and without electrode wire vibrations) and under a flux layer (submerged arc welding), using an electrode wire with a diameter of Ø = 1.6 mm. Table 2 presents the corresponding deposition velocity, voltage, and electrode wire feed rate for the different weld deposition methods.

Table 2

Deposition parameters for different weld deposition methods

Weld deposition method		
CO_2 shielding with wire vibrations	**CO_2 shielding without wire vibrations**	**Under flux layer**
Velocity of weld coating deposition V_{wcd} [m/min]		
1.0	0.8	0.8
Voltage of weld coating deposition U_{wcd} [V]		
20	22	28
Velocity of electrode wire supply V_{ews} [m/min]		
2.3	2.3	2.3

During the preparation of the cross-sections, the samples were polished and etched using a 3% nitric acid solution (nital). Microhardness across the depth was measured on the prepared cross-sections.

Microhardness measurements of the weld overlay coatings were performed using a PMT-3 microhardness tester (Fig. 1a) with a load of 100 g. The measurements were carried out along the thickness of the deposited layer (Fig. 1b). In the near-surface region of the deposited weld metal, the measurement spacing was l_2 = 0.25 mm, while at greater depths it was l_1 = 0.50 mm. In the heat-affected zone (HAZ) and the base metal, the measurement spacing was maintained at l_2 = 0.25 mm.

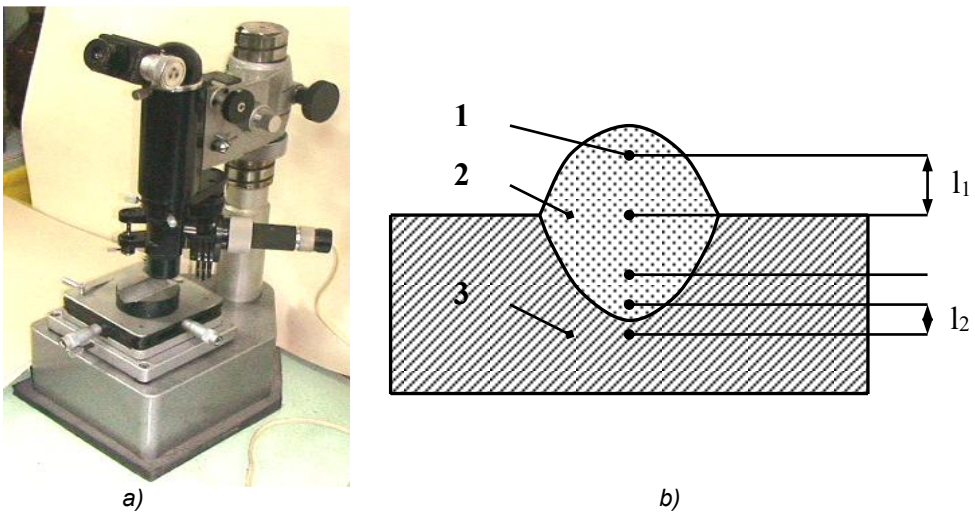

Fig. 1 - Microhardness tester (a) and schematic diagram of the microhardness measurement path (b): 1 – measurement control point; 2 – weld metal; 3 – base metal; l_1 and l_2 – distances between measurement points.

RESULTS AND DISCUSSION

Figure 2 presents one of the specimens with deposited weld coatings.

Fig. 2 – Specimen with deposited weld coating

The variation of the weld deposition current, I_{wcd}, as a function of the electrode wire feed rate, V_{ews}, is presented in Figures 3–5. The increase in welding current with increasing wire feed rate is attributed to the higher heat input required to melt the larger amount of filler metal. A similar trend is observed with increasing electrode wire diameter. An increase in weld deposition current corresponds to an increase in both electrical and thermal power. In general, the highest current values are observed during deposition under a flux layer (submerged arc welding), while the lowest values are obtained during deposition in a CO_2 shielding environment with electrode wire vibrations. In the latter method, the maximum electrode wire diameter cannot be utilized due to technological limitations.

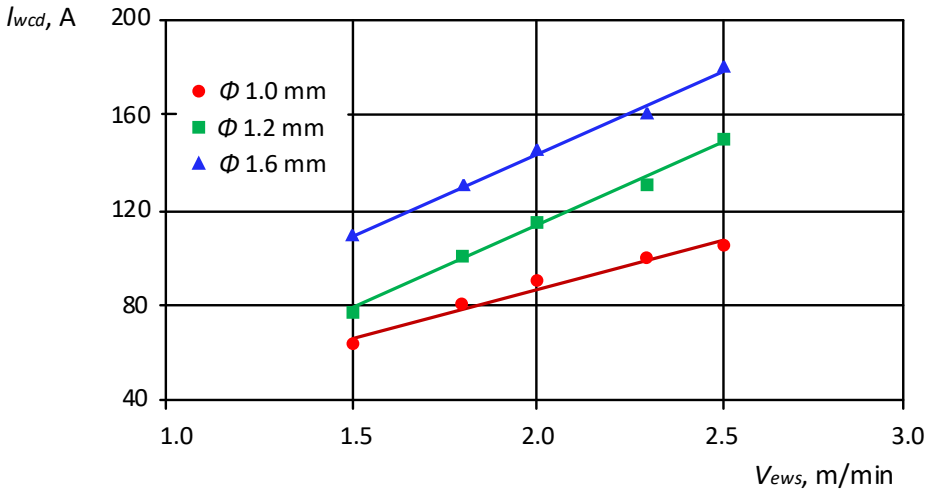

Fig. 3 - Variation of weld deposition current I_{wcd} as a function of electrode wire feed rate V_{ews} during weld deposition under CO_2 shielding gas with electrode wire vibrations

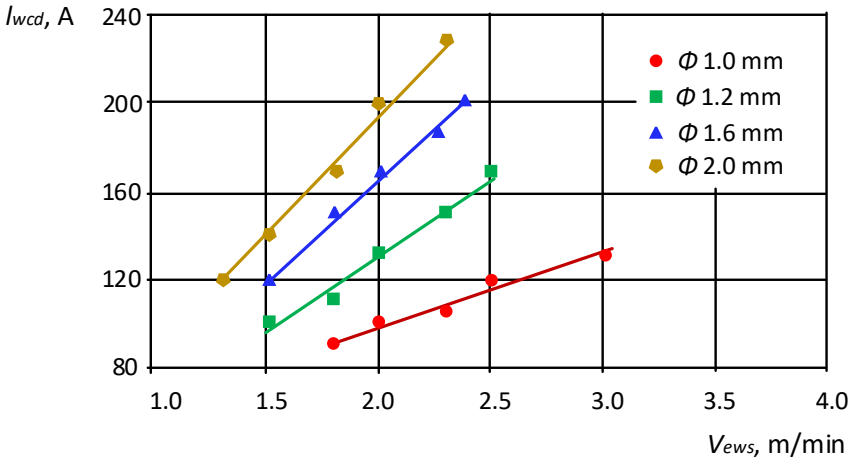

Fig. 4 - Variation of weld deposition current I_{wcd} as a function of electrode wire feed rate V_{ews} during weld deposition under CO_2 shielding gas without electrode wire vibrations

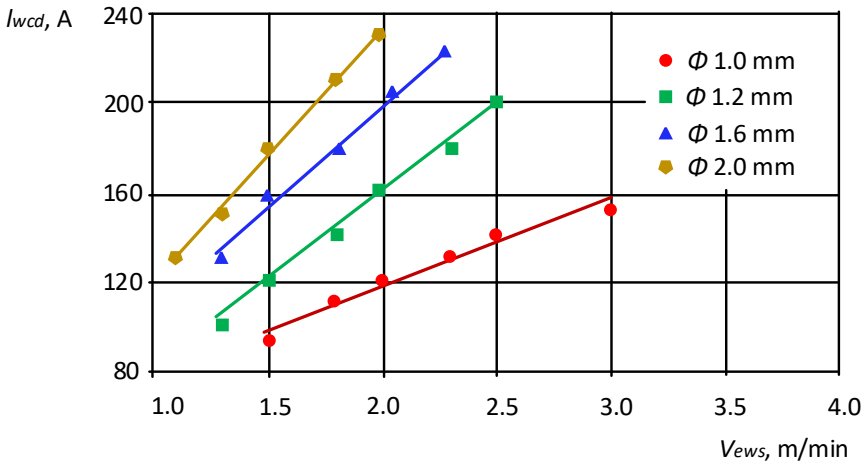

Fig. 5 - Variation of weld deposition current I_{wcd} as a function of electrode wire feed rate V_{ews} during weld deposition under a flux layer

The range of variation of the electrode wire feed rate is determined by identifying the limits at which minimal current fluctuations and proper weld bead formation are ensured (Table 3).

From the results presented in Figures 3–5 and Table 3, it can be observed that the welding current increases with increasing electrode wire feed rate. Depending on the electrode wire diameter and the deposition method, the variation range of the wire feed rate, and consequently the welding current, differs. At the lower limit of the current range, the arc power required for stable ignition and maintenance may be insufficient. Additionally, at low wire feed rates, the self-regulation mechanism of the arc may be disrupted, leading to a rapid increase in arc length and eventual arc extinction. This results in a significant deterioration in process stability and weld bead quality. The upper limit of the current range is reached when the current density attains values that disrupt the arc self-regulation mechanism. In this case, the electrode wire feed rate exceeds the melting rate, leading to process instability.

Table 4 presents summarized results from the statistical analysis conducted to determine the stability limits of the weld deposition processes. High coefficients of determination ($R^2 \geq 0.952$) were obtained for all investigated methods, indicating a strong correlation and high reliability of the proposed linear models. The resulting p-values ($p < 0.001$) confirm that the relationship between welding current and electrode wire feed rate is statistically significant and governed by a consistent physical relationship within the selected operating range. This level of statistical accuracy enables reliable prediction of energy parameters, which is essential for ensuring consistent weld quality in automated deposition processes.

Table 3

Stability limits of weld deposition processes for different methods

Weld deposition method								
CO_2 shielding with wire vibrations			**CO_2 shielding without wire vibrations**			**Under flux layer**		
Ø = 1.0 mm								
V_{ews} [m/min]			**V_{ews} [m/min]**			**V_{ews} [m/min]**		
1.5	2.0	2.5	1.8	2.3	3.0	1.5	2.3	3.0
I_{wcd} [A]			**I_{wcd} [A]**			**I_{wcd} [A]**		
70	90	110	90	110	130	90	130	150
Ø = 1.2 mm								
V_{ews} [m/min]			**V_{ews} [m/min]**			**V_{ews} [m/min]**		
1.5	2.0	2.5	1.5	2.0	2.5	1.5	2.0	2.5
I_{wcd} [A]			**I_{wcd} [A]**			**I_{wcd} [A]**		
80	110	140	100	130	170	80	110	140
Ø = 1.6 mm								
V_{ews} [m/min]			**V_{ews} [m/min]**			**V_{ews} [m/min]**		
1.5	2.0	2.5	1.5	2.0	2.3	1.3	1.8	2.3
I_{wcd} [A]			**I_{wcd} [A]**			**I_{wcd} [A]**		
110	140	180	120	170	200	120	190	200
Ø = 2.0 mm								
V_{ews} [m/min]			**V_{ews} [m/min]**			**V_{ews} [m/min]**		
-	-	-	1.3	1.8	2.3	1.1	1.5	2.0
I_{wcd} [A]			**I_{wcd} [A]**			**I_{wcd} [A]**		
-	-	-	120	170	220	160	200	260

Table 4

Summary of statistical analysis for determining the stability limits of weld deposition processes

Weld deposition method	Wire diameter Ø, mm	Regression equation	R^2	p-value
CO_2 shielding with wire vibrations	1.0	$I_{wcd} = 6.414 + 40.191V_{ews}$	0.972	0.002
	1.2	$I_{wcd} = -27.134 + 70.076V_{ews}$	0.992	< 0.001
	1.6	$I_{wcd} = 8.296 + 67.675V_{ews}$	0.992	< 0.001
CO_2 shielding without wire vibrations	1.0	$I_{wcd} = 31.221 + 33.525V_{ews}$	0.956	0.004
	1.2	$I_{wcd} = -12.102 + 71.338V_{ews}$	0.974	0.002
	1.6	$I_{wcd} = -10.147 + 88.235V_{ews}$	0.990	0.005
	2.0	$I_{wcd} = -26.975 + 111.783V_{ews}$	0.996	< 0.001
Under flux layer	1.0	$I_{wcd} = 37.223 + 39.440V_{ews}$	0.952	0.001
	1.2	$I_{wcd} = -4.151 + 81.132V_{ews}$	0.997	< 0.001
	1.6	$I_{wcd} = 22.739 + 91.720V_{ews}$	0.993	< 0.001
	2.0	$I_{wcd} = 30.008 + 100.011V_{ews}$	0.998	0.001

Figure 6 illustrates the main microstructural constituents of the weld overlay coatings obtained using the investigated deposition methods. The deposited weld metal is located in the upper part of images “a” and “b”, and in the upper-left region of image “c”. Beneath this region, the heat-affected zone (HAZ) and the base metal can be observed.

Table 5 presents the microhardness distribution across the coating depth for the different weld deposition methods. The values corresponding to the HAZ are highlighted in bold.

Figures 7–9 show the variation of microhardness in the deposited metal, the heat-affected zone (HAZ), and the base metal for the investigated weld deposition methods.

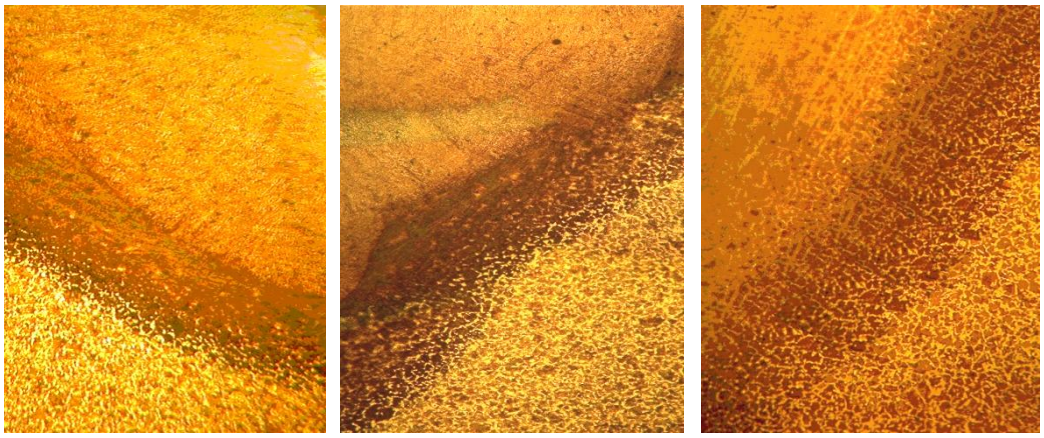

a) *b)* *c)*

Fig. 6 - Metallographic cross-sections at 170x magnification: (a) weld deposition under CO_2 shielding gas with electrode wire vibrations; (b) weld deposition under CO_2 shielding gas without electrode wire vibrations; (c) weld deposition under a flux layer

Table 5

Microhardness distribution across the coating depth for different weld deposition methods

Measurement depth L [mm]	Weld deposition method		
	CO_2 shielding with wire vibrations	CO_2 shielding without wire vibrations	Under flux layer
	Microhardness [HV]		
0.25	321	378	402
0.50	321	378	400
0.75	313	348	389
1.25	321	339	400
1.75	305	348	389
2.25	321	339	389
2.50	340	348	**438**
2.75	**358**	**358**	**451**
3.00	**368**	**390**	**438**
3.25	**358**	**389**	**451**
3.50	**348**	**375**	**412**
3.75	313	**356**	**400**
4.00	231	353	**368**
4.25	241	241	235
4.50	235	258	233
4.75	231	231	231
5.00	235	235	235

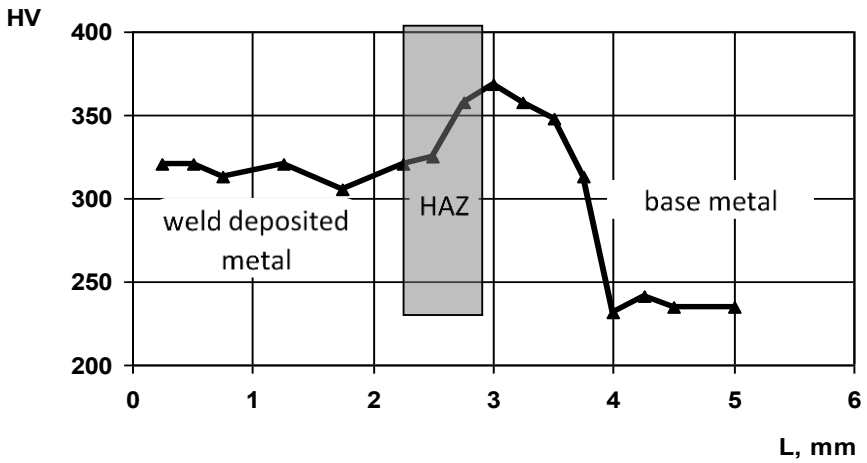

Fig. 7 - Variation of microhardness across the coating depth during weld deposition under CO_2 shielding gas with electrode wire vibrations

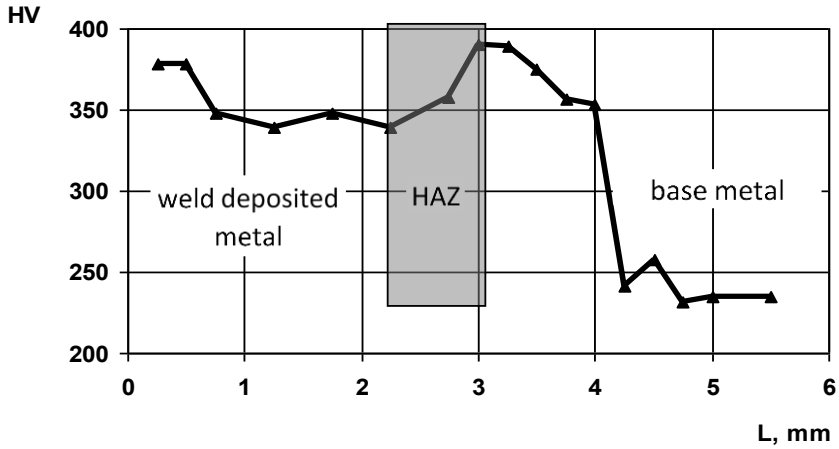

Fig. 8 - Variation of microhardness across the coating depth during weld deposition under CO_2 shielding gas without electrode wire vibrations

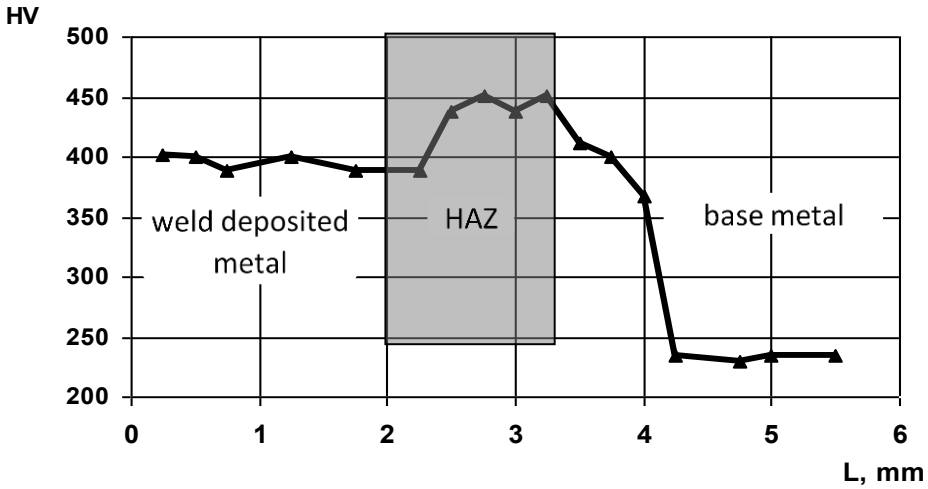

Fig. 9 - Variation of microhardness across the coating depth during weld deposition under a flux layer

The analysis of microhardness results indicates that, during weld deposition under a flux layer, the variation of microhardness within the deposited metal is significantly lower than that observed during deposition under CO_2 shielding gas. This more uniform microhardness distribution is directly related to improved durability of the restored surfaces, depending on the dominant wear mechanism. Higher microhardness values are generally associated with increased wear resistance. The heat-affected zone formed during deposition under a flux layer is larger than that obtained under CO_2 shielding gas. This can be explained by the higher effective arc power associated with submerged arc welding, which results in greater heat input.

In addition to the parameters governing process stability, the welding current is also constrained by the diameter of the component and the length of the weld pool. The allowable weld pool length, L_{wcdp}, is a key limiting parameter in the weld deposition of cylindrical components with different diameters, as it determines the feasibility of applying a given method under specific operating conditions. Only those electrode materials and deposition methods for which the allowable weld pool length, and correspondingly the welding current, fall within the stable operating range are suitable for application. When multiple methods or operating modes are feasible, the preferred choice is the one that ensures the highest productivity. Therefore, it is necessary to establish functional relationships between the controllable process parameters and the limiting factors described above.

CONCLUSIONS

As a result of the experimental investigation carried out using three different methods, the stability limits of weld overlay deposition processes applied to worn cylindrical steel components of agricultural machinery were determined. The lower and upper limits were established with respect to the electrode wire feed rate (from 1.1 m/min to 3.0 m/min, depending on the method and electrode diameter) and the corresponding welding current (from 70 A to 260 A).

It was established that, in general, the highest welding current values, and consequently the greatest thermal input to the restored components, are observed during deposition under a flux layer. One of the contributing factors is the presence of slag formed during flux melting, which acts as thermal resistance and reduces heat dissipation to the environment.

The microstructure and microhardness of the weld overlay coatings obtained by the three investigated methods were analyzed. The results show that the highest microhardness values are generally observed in the heat-affected zone, reaching up to 451 HV for deposition under a flux layer, while the lowest values are found in the base metal (minimum 231 HV). The highest microhardness of the deposited metal is also achieved in the case of deposition under a flux layer (up to 402 HV). Furthermore, for this method, the variation of microhardness across the coating depth is the smallest (13 HV), compared to 35 HV for CO_2 shielding with wire vibrations and 39 HV for CO_2 shielding without wire vibrations. This indicates that deposition under a flux layer provides the highest wear resistance of the deposited metal, as well as greater uniformity of properties across the coating thickness. Consequently, this method ensures more consistent performance when restoring components with varying degrees of wear on their working surfaces.

ACKNOWLEDGEMENT

This study is financed by the European Union-NextGenerationEU, through the National Recovery and Resilience Plan of the Republic of Bulgaria, project № BG-RRP-2.013-0001.

REFERENCES

[1] Bujaczek R., Sławiński K., & Grieger A. (2013). Agricultural machines maintenance and repair services in western Pomerania. *Technical Science*, 16(1). https://uwm.edu.pl/wnt/technicalsc/tech_16_1/b02.pdf

[2] Burose F. & Sauer N. (2011). Repair and maintenance costs – results from a survey. *Man and machinery*, *Landtechnik* ,66(4), 259–263. www.agricultural-engineering.eu

[3] Calcante A., Fontanini L., & Mazzetto F. (2013). Repair and maintenance costs of 4WD tractors and self propelled combine harvesters in Italy. *Journal of Agricultural Engineering*, XLIV(s2):e70, 353–358. https://www.agroengineering.org/jae/article/view/jae.2013.s2.e70

[4] Gehling T., Treutler K., & Wesling V. (2022). Development of surface coatings for high-strength low alloy steel filler wires and their effect on the weld metal microstructure and properties. *Welding in the World*, Published online. https://link.springer.com/article/10.1007/s40194-021-01086-3

[5] Jialin Han, Jiaxiang Zhang, Bing Zeng, & Mingsong Mao (2021). Optimizing dynamic facility location-allocation for agricultural machinery maintenance using Benders decomposition. *Omega*, 105(102498). https://www.sciencedirect.com/science/article/pii/S0305048321001079

[6] Jialin Han, Qian Xiang, Bing Zeng, Yang Lei, & Laishao Luo (2022). A multi-objective dynamic covering location problem for hierarchical agricultural machinery maintenance facilities. *Knowledge-Based Systems*, 252(109462). https://www.sciencedirect.com/science/article/pii/S095070512200733X

[7] Jialin Han, Yaoguang Hu, Mingsong Mao, & Shuping Wan (2020). A multi-objective districting problem applied to agricultural machinery maintenance service network. *European Journal of Operational Research*, 287, 1120–1130. https://www.sciencedirect.com/science/article/pii/S0377221720304197

[8] Jia-qi Shen, Zong-yi Zhang, & Hong-bo Li. (2025). Cost-benefit analysis of remanufacturing of used agricultural machinery parts in China. *Journal of Cleaner Production*, 533(146944). https://www.sciencedirect.com/science/article/pii/S0959652625023005

[9] Lips M. & Burose F. (2012). Repair and maintenance costs for agricultural machines. *International Journal of Agricultural Management*, 1(3). https://www.academia.edu/19039325/Repair_and_Maintenance_Costs_for_Agricultural_Machines

[10] Malykha E.F., Ashmarina T.I., Sergeyeva N.V., & Biryukova T.V. (2023). Formation of a system for the disposal of agricultural machinery in the agro-Industrial transport complex. *Transportation Research Procedia*, 68, 870–875. https://www.sciencedirect.com/science/article/pii/S2352146523001254

[11] Mel´endez-Morales L.D., Ruíz-Mondrag´on J.J., & Hern´andez-Hern´andez M. (2023). In-service weld repair by direct deposition: Numerical simulation and experimental validation. *Engineering Science and Technology, an International Journal*, 46(101503). https://www.sciencedirect.com/science/article/pii/S2215098623001817

[12] Popovych P., Lyashuk O., Shevchuk O., Tson O., Poberezhna L., & Bortnyk I. (2017). Influence of organic operation environment on corrosion properties of metal structure materials of vehicles. *INMATEH Agricultural Engineering*, 52(2), 113–118. https://oaji.net/articles/2017/1672-1515532932.pdf

[13] Pourdarbani R. (2019). Choosing a proper maintenance and repair strategy for tractors (in Urmia). *Acta Technologica Agriculturae* ,1, 12–16. https://reference-global.com/article/10.2478/ata-2019-0003

[14] Vorotnikov I.L., Petrov K.A., Esin O.A. Gutuev M.Sh., & Ermolova O.V. (2019). Organization for repair technology and maintenance of agricultural machinery. *International Journal of Recent Technology and Engineering (IJRTE)*, 8(2). https://www.ijrte.org/portfolio-item/b3511078219/

[15] Voynash S.A., Gaydukova P.A., & Markov A.N. (2017). Rational route choosing methodology for machine parts restoration and repair. *Procedia Engineering*, 206, 1747–1752. https://www.sciencedirect.com/science/article/pii/S1877705817353948

[16] Winczek J., Gucwab M., & Skroński Ł. (2020). Estimation of heat energy in regeneration of agricultural machine parts by welding methods. *Agricultural Engineering*, 24(3), 91–100. https://scispace.com/pdf/estimation-of-heat-energy-in-regeneration-of agricultural-4k3igvd5e5.pdf

[17] Yanhu Zhang, Yuhua Zhou, Jianwei Li, & Hao Fu (2026). Rate-dependent friction in agricultural machinery: Multiscale mechanisms and regulation strategies. *Progress in Engineering Science*, 3(100184). https://www.sciencedirect.com/science/article/pii/S2950425225001367

[18] Yaoguang Hu, Shasha Xiao, Jingqian Wen, & Jinliang Li (2019). An ANP-multi-criteria-based methodology to construct maintenance networks for agricultural machinery cluster in a balanced scorecard context. *Computers and Electronics in Agriculture*, 158, 1–10. https://www.sciencedirect.com/science/article/pii/S0168169917311249

[19] Yaoguang Hu, Yu Liu, Zhe Wang, Jingqian Wen, Jinliang Li, & Jie Lu (2020). A two-stage dynamic capacity planning approach for agricultural machinery maintenance service with demand uncertainty. *Biosystems Engineering*, 190, 201–217. https://www.sciencedirect.com/science/article/pii/S1537511019309171

[20] Yipu Yao, Jingqian Wen, Xiaoyang Zhen, & Yaoguang Hu (2021). A location-allocation model of maintenance resources based on fault distribution for agricultural machinery maintenance service network. *Procedia CIRP*, 104, 393–398. https://www.sciencedirect.com/science/article/pii/S2212827121009641

[21] Zichao Yu, Diqing Fan, Ling Sha, Xintian Liu, & Yuxuan Dai (2024). Process planning of repairing and grinding for cylindrical parts based on surface defect detection. *Measurement Science and Technology*, 36(015434). https://iopscience.iop.org/article/10.1088/1361-6501/ad9ca3